Photogrammetrie • Fernerkundung • Geoinformation 3/2007, S. 187–195, 4 figs., 2 tabs.

Area-based Orientation of Brightness, Range and Intensity Images

AXEL WENDT, Oldenburg und Hannover & CHRISTIAN HEIPKE, Hannover

Keywords: Close range photogrammetry, orientation, surface matching, reconstruction, data fusion, terrestrial laser scanning

Summary: Within the scope of a common evaluation of brightness, range and intensity images, this article introduces a new area-based approach to achieve the simultaneous orientation of these multiple data types. The actual innovation is a model for the combined least-squares adjustment, which is an extension of object space image matching with ranges and intensities as additional observations. The complete mathematical model is specified and discussed. For a representation of complex object surfaces, the simultaneous consideration of multiple surface patches is described. In the experiments, the general feasibility of this approach is proven with a real data set consisting of terrestrial laser scanner and camera data. It is demonstrated, that by simultaneously refining the object surface, the suggested approach yields better results compared to using constant surface information, and that brightness images can be oriented relative to laser scanner data including range and intensity images.

Zusammenfassung: *Flächenbasierte Orientierung von Helligkeits-, Entfernungs- und Intensitätsbildern*. Mit der Zielsetzung der gemeinsamen Auswertung von Helligkeits-, Entfernungs- und Intensitätsbildern wird ein neuer flächenbasierter Ansatz zur simultanen Orientierung der unterschiedlichen Datenarten vorgestellt. Das Neue dabei ist ein Modell zur kombinierten Kleinste-Quadrate Ausgleichung, das eine Erweiterung der objektraumbasierten Bildzuordnung darstellt. Die Entfernungen und Intensitäten werden als zusätzliche Beobachtungen in das Modell miteinbezogen. Das vollständige mathematische Modell wird vorgestellt und diskutiert. Zur Verarbeitung komplexer Oberflächen werden zusätzlich mehrere Oberflächenausschnitte berücksichtigt. In den Experimenten wird die generelle Anwendbarkeit des Ansatzes anhand realer Daten eines terrestrischen Laserscanners und einer Kamera nachgewiesen. Weiter wird gezeigt, dass die simultane Oberflächenrekonstruktion die Orientierungsbestimmung verbessert, und dass Helligkeitsbilder relativ zu Laserscannerdaten, bzw. Entfernungs- und Intensitätsbildern orientiert werden können.

1 Introduction

Documentation of building facades is useful in a variety of applications such as architecture, cultural heritage recording, virtual reality and urban planning. Currently, the standard technique for data capture is terrestrial photogrammetry. In recent times terrestrial laser scanning has gained considerable attention. Also combined sensor systems have been developed, which deliver range and intensity images from a laser scanner and brightness images from a firmly attached camera. In general, the relative orientation between the two sensors of a combined system, consisting of three translations and three rotations, is pre-calibrated and thus known.

These optical measurement techniques provide brightness, range and intensity images. Brightness images contain texture information, range images directly yield geometric information of the depicted scene, see Fig. 1. The intensity images are additionally obtained from the laser scanner and contain the energy of the laser signal, which is reflected back towards the sensor. Due to their

1432-8364/07/2007/0187 $ 2.25

Fig. 1: The potential of different image types. From left to right: Brightness, range and intensity image.

partly different and partly similar characteristics these data types complement each other, but also contain some redundant information.

As is well known, image orientation is a prerequisite for any photogrammetric task involving the transformation between the different sensor data. A new object-based approach for the simultaneous orientation of multiple sensors is presented in this paper. Preliminary work can be found in Wendt & Heipke (2005).

Related work

For the area-based orientation of images taken from different positions several approaches have been developed in photogrammetry and computer vision. A general overview of the orientation of brightness images is given by Heipke (1997). In the context of this paper only object based image matching algorithms are relevant. These algorithms are published in detail in the literature, e. g. Ebner et al. (1987), Wrobel (1987) and Helava (1988). The functional model includes the sensor and orientation parameters and the parameters of the surface function. Kempa (1995) demonstrates the estimation of the image orientation beside the surface reconstruction. Rosenholm & Torlegard (1988) and Strunz (1993) show how to orient aerial images with surfaces in object space. These approaches for brightness image orientation are also relevant for intensity images.

For a general overview concerning range data orientation refer e. g. to Williams et al. (1999) and Grün & Akca (2004). Several approaches have been presented based on the Iterative Closest Point (ICP) algorithm introduced by Besl & McKay (1992), Chen & Medioni (1992) and Zhang (1994). The algorithm directly works with point clouds in object space and assumes that one point set is a subset of the other. The basic idea of the ICP algorithm is that the closest points approximate the true point correspondences. Modifications of this algorithm were developed for multiple point cloud orientation and for increasing the accuracy and reliability of the results, e. g. by giving each point of the cloud additional attributes, like texture (Johnson & Kang 1997). A further extension of the ICP algorithm with regard to the surface description is given by Grün & Akca (2004), where the authors represent the point cloud as a patch-wise surface function. Akca (2005) introduces an extension of this surface matching approach by using additional intensity values and other surface based data. Kraus et al. (2006) modify the least-squares matching for strip adjustment and quality control for airborne laser scanner data by introducing a template matching approach, using height, intensity and slope information.

One weakness of the approaches of range and brightness orientation is the limited use of multi-source data. Additional data is mostly treated as an attribute of the master data source. In our research we deal with

data sets of objects recorded with more than one sensor type and multiple views simultaneously. The goal is to use the full potential of the recorded data for the orientation estimation.

2 The new orientation concept

In this section a new, general approach for the simultaneous orientation of multiple images is introduced. The orientation concept is based on the combination of object based image matching and the exploitation of range and intensity images.

2.1 *The functional model*

For the model description, the definition of the various coordinate systems, the orientation of the individual sensors in object space, the transformation between sensor space and object space and the definition of the object surface must be introduced, see Fig. 2.

In sensor space of the brightness image, the coordinate system $[x',y',z']$ is defined with the origin in the projection centre. For the range image, the sensor system origin $[x^L,y^L,z^L]$ is defined as the centre of the terrestrial laser scanner. In both sensor systems, the x- and y-axis are defined in the row and column direction of the image. The intensity image is related to the same sensor system as the range image. The object surface Z(X,Y) is given in the object space coordinate system [X,Y,Z], e. g. in a grid, defined by four node points for each grid cell and an interpolation function, e. g. bilinear. Within each grid cell a predefined number of surface elements for the grey values G(X,Y) and the intensity values I(X,Y) is defined, see Fig. 2. The exterior orientation of the sensor referring to object space is given by $O^C(\mathbf{T}^C,\mathbf{R}^C)$ for the brightness image and $O^L(\mathbf{T}^L,\mathbf{R}^L)$ for the laser data. The parameters of the orientation consist of three translations $\mathbf{T}(t_X,t_Y,t_Z)$ and three rotations around the X,Y and Z axis, respectively, captured in the rotation matrix $\mathbf{R}(r_{11},r_{12},\ldots,r_{33})$. The relation of a brightness value $g'(x',y')$ in sensor space to the corresponding grey value G(X,Y) of a surface element (X,Y) in object space is also outlined in Fig. 2. The brightness is a function of the image coordinates, which in turn depend on the object coordinates and the image orientation via the collinearity equations.

$$g'(x',y') = G(X,Y) \tag{1}$$

with

$$x' = -c\frac{r_{11}^C\Delta X + r_{21}^C\Delta Y + r_{31}^C\Delta Z}{r_{13}^C\Delta X + r_{23}^C\Delta Y + r_{33}^C\Delta Z} \tag{2}$$

$$y' = -c\frac{r_{12}^C\Delta X + r_{22}^C\Delta Y + r_{32}^C\Delta Z}{r_{13}^C\Delta X + r_{23}^C\Delta Y + r_{33}^C\Delta Z} \tag{3}$$

and

$$\begin{aligned}\Delta X &= X - t_X^C\\ \Delta Y &= Y - t_Y^C\\ \Delta Z &= Z(X,Y) - t_Z^C\end{aligned} \tag{4}$$

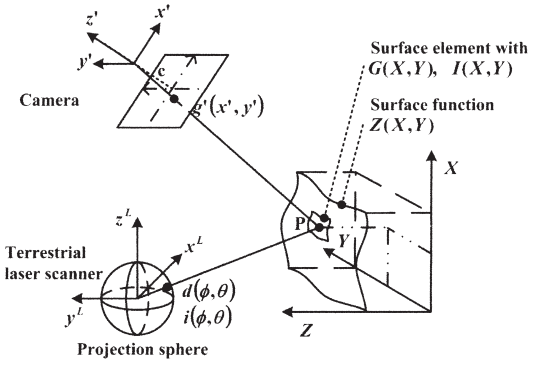

Fig. 2: Parameters of the functional model.

The brightness values in image space vary depending on the light source, surface reflectance and further parameters. Therefore, an illumination and a reflection model have to be included in equation (1). In the case of small parts on the surface a linear transfer function between the brightness value g′ and the grey value G in object space is assumed to be sufficient. Equation (1) then reads:

$$t_0^{g'} + t_1^{g'} \cdot g'(x', y') = G(X, Y) \tag{5}$$

with linear transfer parameters for offset $t_0^{g'}$ and scale $t_1^{g'}$.

The range values of the laser scanner are expressed as distances d in a direction (ϕ, θ) relative to the $[x^L, y^L, z^L]$ system. ϕ is the angle between the x^L-axis and the direction of d projected into the x^L, y^L plane and θ the angle between the direction of d and z^L-axis. The observed range d must then be identical to the distance s between the observed surface point and the origin of the laser scanner:

$$d(\phi, \theta) = s \tag{6}$$

with

$$\phi = \arctan\left(\frac{y^L}{x^L}\right) \tag{7}$$

$$\theta = \arctan\left(\frac{\sqrt{(x^L)^2 + (y^L)^2}}{z^L}\right) \tag{8}$$

$$s = \sqrt{\begin{matrix}(X - t_Z^L)^2 + (Y - t_Y^L)^2 + \\ (Z(X,Y) - t_Z^L)^2\end{matrix}} \tag{9}$$

In order to express ϕ and θ as functions of the object space coordinates [X,Y,Z] and thus establish a relationship between a range value d and the [X,Y,Z] system, the transformation between the range image sensor system and the object space system is necessary:

$$\begin{pmatrix} x^L \\ y^L \\ z^L \end{pmatrix} = (\mathbf{R}^L)^2 \begin{pmatrix} X - t_X^L \\ Y - t_Y^L \\ Z(X,Y) - t_Z^L \end{pmatrix} \tag{10}$$

The intensity value i is also a function of its image coordinates which depend on the object coordinates and the image orientation via the collinearity equations. The relation of an intensity value $i(\phi, \theta)$ to the corresponding reflectance value I(X,Y) of a surface element (X,Y) in object space is given by:

$$i(\phi, \theta) = I(X, Y) \tag{11}$$

In this case the intensity value i is a function of the same image coordinates as the range value. Thus, equations (7), (8) and (10) are also relevant for the functional description of (11). In the same way as the brightness values, also the intensity values in image space vary depending on surface reflectance and further parameters. Again, it is assumed that a linear transfer function is sufficient to consider these effects. Equation (11) then reads:

$$t_0^i + t_1^i \cdot i(\phi, \theta) = I(X, Y) \tag{12}$$

In case of locally noisy or missing image information the introduction of additional constraints for stabilising the object surface is useful. Otherwise, such information may result in wrong surface parameters, and information gaps can lead to singularities in the normal equations. The constraints can be used to minimise curvature, e. g. as suggested by Terzopoulos (1988). In their discrete form they read:

$$\begin{aligned} C_X &= (Z_{r,c-1} - 2Z_{r,c} + Z_{r,c+1}) \\ C_y &= (Z_{r-1,c} - 2Z_{r,c} + Z_{r+1,c}) \\ C_{X,Y} &= \begin{pmatrix} Z_{r,c} - Z_{r+1,c} - Z_{r,c+1} + \\ Z_{r+1,c+1} \end{pmatrix} \end{aligned} \tag{13}$$

with r,c the node point in the row r and column c. C_X, C_Y represents the equations in the direction of the coordinate axis and $C_{X,Y}$ in the diagonal direction. We have implemented these constraints as additional observation equations.

2.2 *Combined sensor system*

In the case of a combined sensor system the relative orientation between the camera and the laser scanner coordinate systems is given by:

$$\mathbf{e} = \mathbf{T}^{L} - \mathbf{T}^{C} \tag{14}$$

$$\mathbf{R}_C^L = \mathbf{R}^L(\mathbf{R}^C)^{-1} = \mathbf{R}^L(\mathbf{R}^C)^T \tag{15}$$

with $\mathbf{e}$ the eccentricity vector between the perspective centres of the camera and laser scanner and $\mathbf{R}_C^L$ the rotation matrix between the two coordinate systems. As the camera is firmly attached to the laser scanner, $\mathbf{e}$ and $\mathbf{R}_C^L$ are known from a calibration step.

2.3 *Simultaneous consideration of multiple surface patches*

So far, the surface in object space has been described with one surface patch only, cf. Fig. 2. In the case of large or complex 3D objects this description may not be sufficient. In this new orientation approach multiple surface patches are introduced, as is shown in Fig. 3.

Each patch j represents a part of the surface with a separate surface function described in a local coordinate system $[X^{Sj},Y^{Sj},Z^{Sj}]$; with j = 1, . . ., n. These patches should be located in areas of geometric surface variation or good brightness texture. The size of each patch can be chosen individually. Without loss of generality the object coordinate system [X,Y,Z] is defined in the first patch, and the orientations of the other patches with respect to the first one are described by the values $\mathbf{O}^{Sj}(\mathbf{T}^{Sj},\mathbf{R}^{Sj})$. For instance, the transformation of the point V^{Sn} of the n^{th} surface patch coordinate system $[X^{Sn},Y^{Sn},Z^{Sn}]$ into the object space coordinate system is given by:

$$\begin{pmatrix} X_V \\ Y_V \\ Z_V \end{pmatrix} = \mathbf{T}^{Sn} + \mathbf{R}^{Sn} \begin{pmatrix} X_V^{Sn} \\ Y_V^{Sn} \\ Z_V^{Sn} \end{pmatrix} \tag{16}$$

2.4 *Adjustment approach*

In the following, the image orientations O, the parameters of the surface function Z(X,Y) as well as the grey values G(X,Y) and reflectance values I(X,Y) of the surface elements, are considered as unknowns. The resulting non-linear observation equations read:

$$\hat{v}_C = \hat{G}(X,Y) - \left(t_0^{g'} + t_1^{g'} \cdot g'\left(\hat{O}^C, \hat{Z}(XY)\right)\right) \tag{17}$$

$$\hat{v}_L = s\left(\hat{O}^L, \hat{Z}(X,Y)\right) - d\left(\hat{O}^L, \hat{Z}(XY)\right) \tag{18}$$

$$\hat{v}_I = \hat{I}(X,Y) - \left(t_0^i + t_1^i \cdot i\left(\hat{O}^L, \hat{Z}(XY)\right)\right) \tag{19}$$

with v_C, v_L, v_I the adjustment residuals. For reasons of simplicity, equations are only given for one surface patch, an extension to

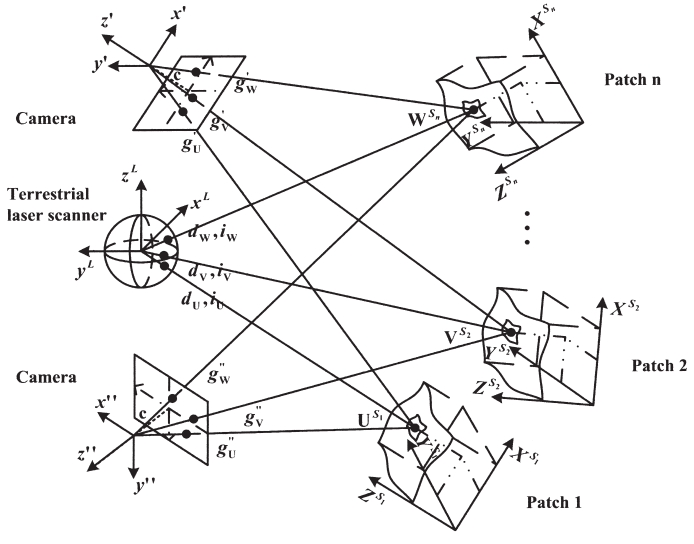

Fig. 3: Simultaneous consideration of multiple surface patches.

multiple patches is straight forward. Also, the additional observation equations for stabilising the surface (see equation (13)) must be added to obtain a solution.

Next, equations (17), (18) and (19) have to be linearised with respect to the unknowns. The adjustment is then solved iteratively using standard formulae. In the case of a combined sensor system data set, the exterior orientation of the brightness images is replaced by the orientations of the laser scanner using equations (14) and (15).

3 Experiments

Experimental testing of the new approach was carried out to demonstrate that:

- Simultaneous adjustment of the different input images and the surface parameters increases the accuracy of sensor orientation for a combined sensor system,
- Individual brightness images can be oriented relative to range and intensity images.

The experiments have been performed using real data. We work in a local object space coordinate system with the origin in one of the laser scanner viewpoints. For the assessment of the results, the root mean square (RMS) values of the different groups of observations in object space are considered. Additionally, the standard deviations of the unknowns of one viewpoint, representing the tendency of all viewpoints, are listed.

3.1 *The test data set*

The orientation is carried out with three viewpoints of the data set *Dresdner Frauenkirche* including brightness, range and intensity images. The data set was recorded with the laser scanner Riegl LSM-Z420i with a mounted Nikon D100 camera. These two sensors can be attached to each other to provide a combined sensor systems, but they can also be operated separately; both options were used in our tests. Effects, like differences in contrast, varying baselines and varying sensor to object distances are present in the data set. For the experiment involving the combined sensor system, calibration values for $\mathbf{e}$ and $\mathbf{R}_C^L$ were determined by a standard procedure recommended by the manufacturer. Sensor orientation values estimated with a feature based orientation concept according to Wendt (2007) were introduced as initial values. For the orientation test twelve surface patches distributed on the facade were chosen, cf. Fig. 3. The average distance between the laser scanner stations and the facade amounts to 45 m.

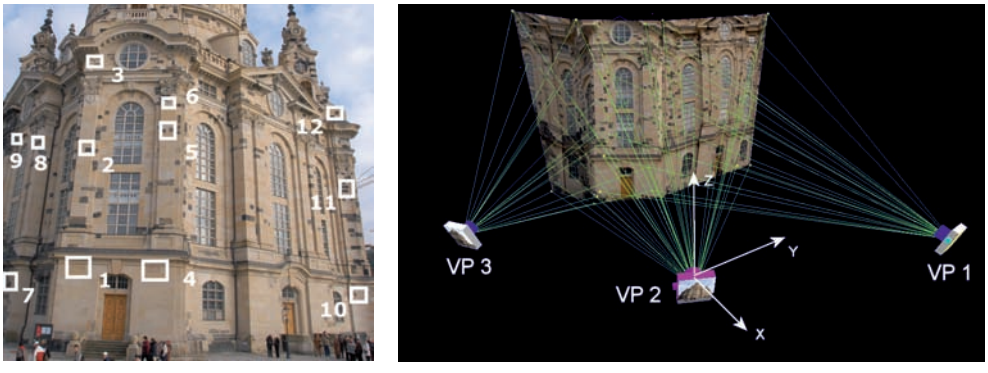

(a) Patch distribution (b) Viewpoints

Fig. 4: Test data setup. (a) shows the surface patch distribution on the facade. Patches 1 to 6 in the centre are observed from 3 viewpoints and patches 7 to 9 and 10 to 12 on either side from 2 viewpoints. (b) shows a sketch of the data acquisition incl. some image rays. From each viewpoint brightness, range and intensity images were captured. Further, the origin of the object space coordinate system (defined in viewpoint 2) together with the coordinate axes is depicted.

These patches lie in approximately planar areas with adequate texture. The size of the patches is chosen according to planarity and texture on the facade and ranges from $0.60\,\text{m} \times 0.72\,\text{m}$ to $1.20\,\text{m} \times 1.20\,\text{m}$. The patches are modeled with a geometric grid size of 0.12 m. The resolution of the range and intensity image is about 0.04 m and of the brightness image about 0.02 m in object space. These values were used to select the size of the surface elements in object space, i.e. the geometric grid mesh of $0.12\,\text{m} \times 0.12\,\text{m}$ consisted of 6×6 surface elements for the grey values and of 3×3 surface elements for the intensity and the distance data. The accuracy for a single range measurement is specified with 0.01 m by the manufacturer. The test, with its planar geometric characteristics represents a typical case in facade modelling. The data set contains problematic aspects: the range images are a little noisy and the intensity images contain a lot of noise. All images include occlusions, because of the different perspective views. These effects are considered by introducing different weights for the observations and the stabilizing functions for the surface reconstruction: The range and brightness observations are used with the weight of 1, the intensity observations with a weight of 1/1000. The stabilizing functions were considered with a weight of 1/10. These weights were chosen after analysing a number of experimental tests, they reflect the relative accuracy of the related observations. In the following three adjustments are carried out:

1. Combined sensor system orientation, surface known
2. Combined sensor system orientation, surface unknown
3. Individual sensor orientation, surface unknown.

In case 1, the surface of the patches is given by the range image of the second viewpoint, and is not refined within the adjustment. For the orientation brightness, range and intensity images are used simultaneously. In case 2, the surface and the orientation parameters of the combined sensor system viewpoints are estimated simultaneously using all three image types. In case 3, the camera is treated as an individual sensor. All three brightness images are oriented relative to the range and intensity images without making use of the calibration values.

All calculations were successful. The iterations were stopped when each change of unknowns caused less than 1/10 pixel change in image space. In Tab. 1 the resulting root mean square values of the grey, the distance, and the intensity values in object space from the three adjustment runs are shown. Additionally, the minimum and maximum height changes of case 2 and case 3 compared to case 1 are listed. Tab. 2 summarises the theoretical standard deviations of the orientation parameter of the first viewpoint in all three cases.

The simultaneous reconstruction of the surface (case 2) compared to the given surface (case 1) leads to an accuracy improvement for the brightness, range and intensity

Tab. 1: RMS values of the different groups of observations in object space and height changes of the surface patches.

	RMS C [0 ... 255]	RMS L [m]	RMSI [0 ... 1]	min/max ΔZ [m]
1	12.9	0.017	0.008	–
2	6.4	0.013	0.005	– 0.080/0.048
3	4.5	0.015	0.006	– 0.030/0.037

Tab. 2: Theoretical standard deviations of the orientation parameters of the first viewpoint.

	1	2	3 scanner	3 camera
S_{Tx} [m]	1.58e-004	1.16e-004	4.74e-004	2.85e-004
S_{Ty} [m]	4.01e-004	2.93e-004	6.33e-004	3.45e-004
S_{Tz} [m]	5.14e-004	3.77e-004	14.18e-004	3.55e-004
S_{Rx} [rad]	1.87e-006	1.38e-006	5.11e-006	2.50e-006
S_{Ry} [rad]	5.71e-006	4.20e-006	15.23e-006	4.11e-006
S_{Rz} [rad]	3.92e-006	2.86e-006	7.61e-006	3.79e-006

values. Also, the theoretical standard deviations of the estimated orientation parameters could be improved. The height changes of the surface patches are within the range of − 0.080 m and 0.048 m. In case 3, where the camera sensor is treated separately from the laser scanner the RMS value for the brightness decreases further, but they increase for the range and intensity values, probably due to the horizontal direction of the surface normals of the more or less planar patches. Thus, in particular, in the Z-direction (the vertical direction, cf. Fig. 4) and the rotation around the Y-axis, being highly correlated to the translation in Z, less orientation information is available, resulting in larger theoretical standard deviations. In contrast, the brightness images contain also orientation information in the Z-direction and for the rotation around Y. This is confirmed by the standard deviations for the orientation parameters. The height chan-ges are between − 0.030 m and 0.037 m. The differences compared to case 2 are compensated by the orientation parameters of the sensors: The relative orientation parameters between the camera and the laser scanner deviate from the calibration values in the dimension of the height differences (about 0.04 m in **e**). The most accurate orientation results are obtained in case 2, where all observations are used to reconstruct the surface and estimate the orientation parameters of a combined sensor system simultaneously.

4 Conclusions

In this paper a new area-based approach for the simultaneous orientation of brightness, range and intensity images and the object surface has been presented, given input data from a terrestrial laser scanner and a digital camera. The approach is based on a non-linear least squares adjustment and extends the object-based image matching method. Using data depicting the Frauenkirche in Dresden the approach is shown to yield good results using multiple surface patches. Further, if orientation and surface are reconstructed simultaneously from all input data, more accurate results are obtained as compared to only computing the orientation. It is also demonstrated that individual brightness images not connected to the laser scanner can be orientated relative to the range and intensity images. In future work more investigations into the pre-requisites concerning texture and geometric surface roughness, the necessary distribution of surface patches and the convergence radius and the numeric stability of the suggested solution will be performed. Another research target is to apply this approach to data sets with varying characteristics to assess the flexibility and generality of the suggested approach.

Acknowledgement

The authors would like to thank Mr. Nikolaus Studnicka from RIEGL GmbH for providing the data set *Dresdner Frauenkirche*.

References

Akca, D., 2005: Registration of point clouds using range and intensity information. – In: Grün, A., Gool, L.V., Pateraki, M. & Baltsavias, M. (Eds.): International Workshop on Recording, Modeling and Visualization of Cultural Heritage. – Taylor & Francis, Leiden pp. 115–126.

Besl, P. & McKay, N., 1992: A method for registration of 3-D shapes. – IEEE Transactions on Pattern Analysis Machine Intelligence, 14(2): 239–256.

Chen, Y. & Medioni, G., 1992: Object modelling by registration of laser scanner data. – Image and Vision computing, 10(3): 145–155.

Ebner, H., Fritsch, D., Gillessen, W. & Heipke, C., 1987: Integration von Bildzuordnung und Objektrekonstruktion innerhalb der digitalen Photogrammetrie. – BuL 55(5): 194–203.

Grün, A. & Akca, D., 2004: Least squares 3D surface matching. – IAPRS, 34(5/W16), (on CD-ROM).

Heipke, C., 1997: Automation of interior, relative, and absolute orientation. – ISPRS Journal of Photogrammetry & Remote Sensing 52: 1–19.

Helava, U.V., 1988: Object-space least-squares correlation. – Photogrammetric Engineering & Remote Sensing 54(6): 711–714.

Johnson, A. & Kang, S., 1997: Registration and Integration of Textured 3-D Data. – International Conference on Recent Advances in 3-D Digital Imaging and Modeling, pp. 234–241.

Kempa, M., 1995: Hochaufgelöste Oberflächenbestimmung von Natursteinen und Orientierung von Bildern mit dem Facetten-Stereosehen. – Dissertation, Technische Hochschule Darmstadt, Darmstadt.

Kraus, K., Ressl, C. & Roncat, A., 2006: Least squares matching for airborne laser scanner data. – In: Gründig, L. & Altan, O. (ed.): Fifth International Symposium Turkish-German Joint Geodetic Days 'Geodesy and Geoinformation in the Service of our Daily Life' ISBN 3-9809030-4-4, p. 7.

Rosenholm, D. & Torlegard, K., 1988: Three-dimensional absolute orientation of stereo models using digital elevation models. – Photogrammetric Engineering & Remote Sensing 54(10): 1385–1389.

Strunz, G., 1993: Bildorientierung und Objektrekonstruktion mit Punkten, Linien und Flächen. – Dissertation, Deutsche Geodätische Kommission, Reihe C, Heft Nr. 408, München.

Terzopoulos, D., 1988: The computation of visible-surface representations. – IEEE Transactions on Pattern Analysis Machine Intelligence 10(4): 417–438.

Wendt, A. & Heipke, C., 2005: A concept for the simultaneous orientation of brightness and range images. – In: Grün, A., Gool, L.V., Pateraki, M. & Baltsavias, M. (eds.): International Workshop on Recording, Modeling and Visualization of Cultural Heritage, Ascona, Switzerland, May 22–27, Taylor & Francis/Balkema, Leiden, pp. 451–457.

Wendt, A., 2007: A concept for feature based data registration by simultaneous consideration of laser scanner data and photogrammetric images. – ISPRS Journal of Photogrammetry & Remote Sensing. (in print)

Williams, J., Bennamoun, M. & Latham, S., 1999: Multiple view 3D registration: A review and a new technique. – IEEE Int. Conf. on Systems, Man, and Cybernetics, Tokyo, pp. 497–502.

Wrobel, B., 1987: Facets stereo vision (fast vision) – a new approach to computer stereo vision and to digital photogrammetry. – In: Fast Processing of Photogrammetric Data. ISPRS Intercommission conference, pp. 231–258.

Zhang, Z., 1994: Iterative point matching for registration of free-form curves and surfaces. – International Journal of Computer Vision 13(2): 119–152.

Addresses of the authors:

Dipl.-Ing. Axel Wendt
Institut für Angewandte Photogrammetrie und Geoinformatik, Fachhochschule Oldenburg/Ostfriesland/Wilhelmshaven
Ofener Str. 16, D-26121 Oldenburg
Tel.: 0441-7708-3606, Fax: 0441-7708-3170
e-mail: a.wendt@fh-oldenburg.de; und
Institut für Photogrammetrie und GeoInformation, Leibniz Universität Hannover
Nienburger Str. 1, D-30167 Hannover

Prof. Dr.-Ing. Christian Heipke
Institut für Photogrammetrie und GeoInformation, Leibniz Universität Hannover
Nienburger Str. 1, D-30167 Hannover
Tel.: 0511-762-2482, Fax: 0511-762-2483
e-mail: heipke@ipi.uni-hannover.de

Manuskript eingereicht: Januar 2007
Angenommen: Januar 2007